Bioorganic & Medicinal Chemistry 18 (2010) 8226–8234

Contents lists available at ScienceDirect

Bioorganic & Medicinal Chemistry

journal homepage: www.elsevier.com/locate/bmc

Rubiyunnanins C–H, cytotoxic cyclic hexapeptides from *Rubia yunnanensis* inhibiting nitric oxide production and NF-κB activation

Jun-Ting Fan [a,b], Jia Su [a,b], Yan-Min Peng [b,c], Yan Li [a], Jia Li [c], Yu-Bo Zhou [c], Guang-Zhi Zeng [a], He Yan [a,b], Ning-Hua Tan [a,*]

[a] State Key Laboratory of Phytochemistry and Plant Resources in West China, Kunming Institute of Botany, Chinese Academy of Sciences, Kunming 650204, PR China
[b] Graduate School of Chinese Academy of Sciences, Beijing 100039, PR China
[c] National Centre for Drug Screen, Shanghai Institute of Materia Medica, Chinese Academy of Sciences, Shanghai 201203, PR China

ARTICLE INFO

Article history:
Received 11 August 2010
Revised 5 October 2010
Accepted 5 October 2010
Available online 31 October 2010

Keywords:
Rubia yunnanensis
Rubiyunnanins C–H
Cyclopeptides
Cytotoxicity
Inhibition of NO production
NF-κB pathway inhibitors

ABSTRACT

Six new (rubiyunnanins C–H, **1–6**) and five known (**7–11**) cyclic hexapeptides were isolated from the roots of *Rubia yunnanensis* (Franch.) Diels. The structures and stereochemistry of **1–6** were established by extensive spectroscopic analyses and chemical methods. All compounds (**1–11**) not only exhibited cytotoxic activities against a panel of eleven cancer cell lines with IC_{50} values ranging from 0.001 to 56.24 μM, but also exerted inhibitory activities against nitric oxide (NO) production in LPS and IFN-γ-induced RAW 264.7 murine macrophages with IC_{50} values ranging from 0.05 to 12.68 μM. Furthermore, this is the first time it is being reported that compounds **2** and **7–10** significantly inhibited TNF-α-induced NF-κB activation in HEK-293-NF-κB luciferase stable cells with IC_{50} values of 35.07, 0.03, 1.69, 12.64 and 1.18 μM, respectively.

1. Introduction

Rubia yunnanensis (Franch.) Diels (Rubiaceae, Chinese name 'Xiao-Hong-Shen'), is a perennial herb native to Yunnan province, China. Its roots have a long history of use in Chinese traditional medicine for the treatment of tuberculosis, menoxenia, rheumatism, contusion, hematemesis, anemia and lipoma.[1] Previous studies have shown that rubiaceae-type bicyclic hexapeptides (RA-series cyclopeptides, RAs),[2–4] anthraquinones[5–8] and arborinane-type triterpenoids[9–14,8] are the major types of chemical constituents of this plant. Within these chemical constituents, RAs have attracted great interest in terms of their distinctive bicyclic structural feature and significant antitumor activities in vivo and in vitro.[15,16] RAs are homodicyclohexapeptides mainly formed with one D-α-alanine, one L-α-alanine, three modified *N*-methyl-L-α-tyrosines and an additional L-α-amino acid. The most unusual feature is a 14-membered ring formed by a phenolic oxygen linkage between two adjacent tyrosines with a *cis* peptide bond, and the 14-membered ring which is fused to a 18-membered cyclic hexapeptide ring.[17] Bouvardin and deoxybouvardin were the first two RAs, isolated from the stems, leaves and flowers of *Bouvardia ternifolia* (Rubiaceae) in 1977.[18] Subsequently, other 28 RAs have been reported from three *Rubia* plants, that is, *Rubia cordifolia*, *Rubia akane* and *Rubia yunnanensis*.[17,19–21] Recently, two novel cyclic peptides named rubiyunnanins A and B from *R. yunnanensis*, were reported from our laboratory.[22] Preliminary studies on antitumor mechanism of RAs indicated that bouvardin and RA-VII inhibited protein synthesis through interaction with eukaryotic ribosomes.[23–25] Furthermore, RA-V and RA-XII have been reported to significantly inhibit overproduction of NO and induction of inducible nitric oxide synthase (iNOS).[8] Recently, RA-VII has been reported to change the conformational structure of F-actin to induce G_2 arrest and exhibit anti-angiogenic activity both in vivo and vitro.[26,27] Moreover, a possible biosynthetic pathway for RAs was proposed, predicting that RAs could be synthesized via a non-ribosomal peptide biosynthetic mechanism.[17,28] In our investigation on structurally interesting cyclopeptides from *R. yunnanensis* and further antitumor mechanism of RAs, six new (rubiyunnanins C–H, **1–6**) and five known (**7–11**) RAs were isolated from the titled plant roots. Herein, their isolation, structural elucidation, cytotoxic activities and inhibitory activities against NO production in LPS and IFN-γ-induced RAW 264.7 murine macrophages were described. Mostly importantly, it was the first time to report that RAs potently inhibit TNF-α-induced NF-κB activation in HEK-293-NF-κB luciferase stable cells.

* Corresponding author. Tel.: +86 871 5223800; fax: +86 871 5223800.
E-mail address: nhtan@mail.kib.ac.cn (N.-H. Tan).

0968-0896/$ - see front matter © 2010 Elsevier Ltd. All rights reserved.
doi:10.1016/j.bmc.2010.10.019

2. Results and discussion

2.1. Structure determination

The methanol extract of the air-dried and powdered roots of *R. yunnanensis* (100 kg) was suspended in water and then partitioned successively with EtOAc and *n*-BuOH. The EtOAc layer was repeatedly chromatographed over a series of silica gel, RP-18 silica gel, Sephadex LH-20 and ODS HPLC to afford eleven RAs (Fig. 1). These included six new ones (rubiyunnanins C–H, **1–6**) and five known ones, RA-V (**7**), RA-I (**8**), RA-XXIV (**9**), RA-XII (**10**), RY-II (**11**).

Rubiyunnanin C (**1**) was obtained as a white crystal. Its molecular formula was established as $C_{43}H_{52}N_6O_{11}$ by its positive HRFABMS (*m/z* 828.3713, $[M]^+$), indicating 21 degrees of unsaturation. Its UV spectrum showed the existence of phenyl groups based on the absorptions at 203 and 277 nm. The IR spectrum exhibited absorption bands at 3414 and 1660 cm^{-1} ascribable to OH, NH and CO groups. The ^1H and ^{13}C NMR spectra of **1** in C_5D_5N (Table 1) displayed characteristics of typical RAs and demonstrated the presence of two conformers in a ratio of 74:26.[29,30] Further analysis of 1D and 2D NMR spectral data of **1** displayed the major conformer's signals for two methyls (δ_H/δ_C 1.35/19.2, 1.54/21.8), three amide *N*-methyl signals (δ_H/δ_C 3.00/30.4, 3.02/29.7, 3.26/40.1), two *O*-methyl signals (δ_H/δ_C 3.51/51.5, 3.66/55.2), five methylenes (δ_H/δ_C 2.36/27.0; 2.56/30.3; 2.61, 3.66/ 36.8; 3.32, 3.56/36.3; 3.85, 3.92/33.9), six α-amino methines (δ_H/δ_C 4.13/68.9, 5.01/58.0, 5.09/46.9, 5.16/48.3, 5.32/48.4, 5.75/54.5), two 1,4-disubstituted benzene rings (δ_C 131.9, 158.9 and δ_H/δ_C 7.00/114.5 × 2, 7.32/130.8 × 2; δ_C 136.1, 158.9 and δ_H/δ_C 6.90/124.7, 6.95/126.6, 7.19/130.9, 7.44/133.5), one 1,2,4-trisubstituted benzene ring (δ_C 128.1, 145.5, 152.8 and δ_H/δ_C 4.64/115.1, 6.75/122.1, 7.21/117.9), seven carbonyl signals (δ_C 168.6, 169.9, 171.3, 172.1, 172.6, 173.0, 173.2) and three amide protons (δ_H 7.36, 8.81, 9.91). An extensive comparison of 1D and 2D NMR spectra data of **1** with those of RA-XXIV (**9**)[21] in C_5D_5N indicated that both compounds were very similar, except for the resonances due to those of the second amino acid residue (AA^2). In the $^1H-^1H$ COSY spectrum, cross-peaks of H-2α/H-2β, NH-2 and H-2β/H-2γ suggested that C-2α was further extended by two methylene carbons at C-2β and C-2γ. The observed HMBC correlations of H-2β, H-2γ and the methoxyl group (δ_H 3.51) with C-2δ (δ_C 173.2) indicated that **1** had a glutamic acid γ-methyl ester unit as AA^2 (Fig. 2). In addition, the upfield shifts of the ^{13}C NMR signals of C-2α, C-2β, C-2γ and C-2δ compared with those of **9**, together with the MS information also corroborated **1** was an analog of **9** whose glutamine was replaced by glutamic acid γ-methyl ester. Moreover, the sequence of the amino acid residues in **1** was confirmed from the HMBC correlations of Glu γ-methyl ester^2-NH/Ala^1-CO, Tyr^3-NMe/Glu γ-methyl ester^2-CO, Ala^4-NH/Tyr^3-CO, Tyr^5-NMe/Ala^4-CO, Tyr^6-NMe/Tyr^5-CO and Ala^1-NH/Tyr^6-CO (Fig. 2). In the ROESY spectrum, NOE correlations were observed between Tyr^3-NMe/H-2α, H-3α, Tyr^5-NMe/H-4α and H-5α/H-6α, indicating the *N*-methyl peptide bonds between Glu γ-methyl ester^2/Tyr^3, Ala^4/Tyr^5 and Tyr^5/Tyr^6 were *trans*, *trans* and *cis*, respectively. Furthermore, crucial NOE correlations of H-1α/H-4β, H-6α/H-6δb, H-6δb/H-5εa were also observed, revealing the similar relative configuration to that of RAs (Fig. 3). The absolute configurations of Ala^1 and Ala^4 were identified as D (*R*) and L (*S*), respectively, by application of the Marfey's method.[31] The remaining configurations of Glu γ-methyl ester^2, Tyr^3, Tyr^5 and Tyr^6 in **1** were determined to be L (*S*), L (*S*), L (*S*) and L (*S*), respectively, by analyzing information from the similar NOE correlations, carbon and proton chemical shifts and proton coupling constants, compared with those of **9**. Accordingly, the structure of **1** was determined as shown in Figure 1.

Rubiyunnanin D (**2**) and rubiyunnanin E (**3**) were obtained as white powders. Compound **2** had the molecular formula $C_{41}H_{48}N_6O_{11}$, established from the positive HRESIMS (*m/z* 823.3259, $[M+Na]^+$), indicating 21 degrees of unsaturation. Compound **3** had the molecular formula $C_{42}H_{50}N_6O_{12}$ by its positive HRESIMS (*m/z* 853.3391, $[M+Na]^+$), corresponding to 21 degrees of unsaturation. The ^1H and ^{13}C NMR spectra of **2** and **3** in C_5D_5N (Table 1) also displayed characteristics of typical RAs and demonstrated the presence of two conformers in a ratio of 78:22 and 77:23, respectively. Comparison of the 1D and 2D NMR spectra of **2** in C_5D_5N with those of **1** showed their structural similarities. The main difference between **2** and **1** was the absence of two *O*-methyl groups. In the ^{13}C NMR spectra of **1** and **2**, the C-2α, C-2β, C-2γ and C-2δ resonances were shifted downfield from δ_C 48.4, 27.0, 30.3, 173.2 in **1** to δ_C 48.8, 27.4, 31.0, 175.4 in **2**, which revealed the replacement of the methoxyl group (δ_C 51.5) in **1** by a hydroxyl group in **2** at the C-2δ position. Moreover, the upfield shifts of C-3γ and C-3ζ from δ_C 131.9 and 158.9

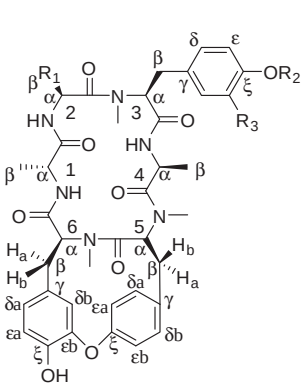

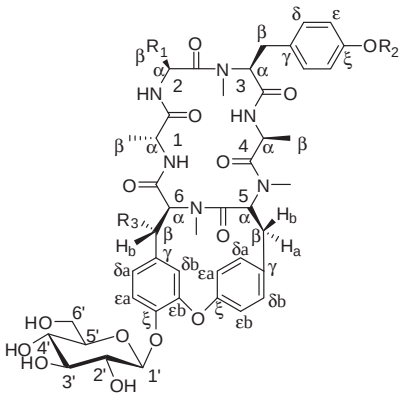

	R_1	R_2	R_3
1	$CH_2CH_2COOCH_3$	CH_3	H
2	CH_2CH_2COOH	H	H
3	CH_2CH_2COOH	CH_3	OH
7	CH_3	CH_3	H
8	CH_2OH	CH_3	H
9	$CH_2CH_2CONH_2$	CH_3	H

	R_1	R_2	R_3
4	$CH_2CH_2CONH_2$	CH_3	H
5	CH_3	H	H
6	CH_3	CH_3	OH
10	CH_3	CH_3	H
11	CH_2OH	CH_3	H

Figure 1. Chemical structures for compounds **1–11**.

Table 1
^{1}H NMR and ^{13}C NMR data for compounds **1**–**3** in C_5D_5N (δ in ppm, J in Hz)

		1		**2**		**3**	
		δ_H[a]	δ_C[b]	δ_H[a]	δ_C[b]	δ_H[a]	δ_C[b]
D-Ala[1]	α	5.16 (q, 7.0)	48.3 d	5.17 (m)	48.4 d	5.17 (m)	48.3 d
	β	1.54 (d, 7.0)	21.8 q	1.55 (d, 6.5)	21.9 q	1.55 (d, 7.0)	21.9 q
	C=O		173.0 s		173.2 s		173.3 s
	NH	8.81 (d, 8.0)		8.80 (d, 8.0)		8.82 (d, 8.0)	
AA[2]	α	5.32 (dd, 15.3, 8.0)	48.4 d	5.44 (dd, 15.3, 8.0)	48.8 d	5.45 (dd, 15.3, 8.0)	48.8 d
	β	2.36 (m)	27.0 t	2.48 (m)	27.4 t	2.46 (m), 2.53 (m)	27.3 t
	γ	2.56 (m)	30.3 t	2.75 (m)	31.0 t	2.75 (m)	31.0 t
	δ		173.2 s		175.4 s		175.4 s
	C=O		172.6 s		172.9 s		172.9 s
	NH	9.91 (d, 8.5)		9.92 (d, 8.5)		9.94 (d, 8.0)	
	OMe	3.51 (s)	51.5 q				
Tyr[3]	α	4.13 (dd, 10.5, 4.5)	68.9 d	4.11 (dd, 10.5, 4.5)	69.1 d	4.16 (dd, 9.3, 5.8)	68.9 d
	βa	3.85 (dd, 13.8, 4.5)	33.9 t	3.89 (m)	34.0 t	3.89 (m)	34.4 t
	βb	3.92 (dd, 13.8, 10.5)					
	γ		131.9 s		130.2 s		133.2 s
	δa	7.32 (d, 8.5)	130.8 d	7.34 (overlap)	131.1 d	7.31 (d, 1.5)	117.7 d
	δb	7.32 (d, 8.5)	130.8 d	7.34 (overlap)	131.1 d	6.90 (overlap)	120.7 d
	εa	7.00 (d, 8.5)	114.5 d	7.22 (overlap)	116.6 d		148.4 s
	εb	7.00 (d, 8.5)	114.5 d	7.22 (overlap)	116.6 d	6.97 (d, 8.5)	112.8 d
	ζ		158.9 s		157.7 s		147.5 s
	C=O		168.6 s		168.9 s		169.0 s
	NMe	3.26 (s)	40.1 q	3.30 (s)	40.2 q	3.31 (s)	40.2 q
	OMe	3.66 (s)	55.2 q			3.68 (s)	56.0 q
Ala[4]	α	5.09 (m)	46.9 d	5.09 (m)	47.0 d	5.09 (m)	47.0 d
	β	1.35 (d, 7.0)	19.2 q	1.36 (d, 6.5)	19.3 q	1.36 (d, 7.0)	19.2 q
	C=O		172.1 s		172.2 s		172.3 s
	NH	7.36 (d, 7.5)		7.37 (d, 8.0)		7.37 (d, 8.0)	
Tyr[5]	α	5.75 (dd, 11.5, 3.0)	54.5 d	5.75 (d, 11.0)	54.6 d	5.75 (dd, 11.5, 3.0)	54.6 d
	βa	2.61 (dd, 11.5, 3.0)	36.8 t	2.62 (d, 11.0)	36.9 t	2.62 (dd, 11.5, 3.0)	36.9 t
	βb	3.66 (overlap)		3.63 (t, 11.0)		3.63 (t, 11.5)	
	γ		136.1 s		136.1 s		136.1 s
	δa	7.44 (dd, 8.5, 2.0)	133.5 d	7.43 (d, 8.0)	133.6 d	7.43 (dd, 8.5, 2.0)	133.6 d
	δb	7.19 (overlap)	130.9 d	7.22 (overlap)	131.1 d	7.25 (overlap)	131.1 d
	εa	6.90 (overlap)	124.7 d	6.89 (br d, 8.0)	124.7 d	6.90 (overlap)	124.7 d
	εb	6.95 (dd, 8.3, 2.5)	126.6 d	6.98 (br d, 8.0)	126.7 d	7.00 (dd, 8.3, 2.0)	126.7 d
	ζ		158.9 s		159.0 s		159.1 s
	C=O		169.9 s		170.0 s		170.0 s
	NMe	3.00 (s)	30.4 q	3.00 (s)	30.5 q	3.00 (s)	30.5 q
Tyr[6]	α	5.01 (dd, 12.3, 3.0)	58.0 d	5.01 (br d, 12.0)	58.1 d	5.02 (dd, 11.8, 3.0)	58.1 d
	βa	3.56 (dd, 17.5, 3.0)	36.3 t	3.55 (br d, 17.5)	36.4 t	3.56 (dd, 18.5, 3.0)	36.4 t
	βb	3.32 (m)		3.30 (overlap)		3.31 (overlap)	
	γ		128.1 s		128.2 s		128.2 s
	δa	6.75 (br d, 8.5)	122.1 d	6.74 (br d, 8.0)	122.2 d	6.74 (br d, 8.0)	122.2 d
	δb	4.64 (br s)	115.1 d	4.66 (br s)	115.2 d	4.69 (br s)	115.3 d
	εa	7.21 (d, 8.5)	117.9 d	7.22 (overlap)	117.9 d	7.19 (overlap)	117.9 d
	εb		152.8 s		152.8 s		152.8 s
	ζ		145.5 s		145.5 s		145.5 s
	C=O		171.3 s		171.4 s		171.4 s
	NMe	3.02 (s)	29.7 q	3.00 (s)	29.8 q	3.00 (s)	29.8 q

[a] Data were measured at 500 MHz.
[b] Data were measured at 125 MHz.

in **1** to δ_C 130.2 and 157.7 in **2**, as well as the downfield shifts of C-3δ and C-3ε from δ_C 130.8 and 114.5 in **1** to δ_C 131.1 and 116.6 in **2** further confirmed the replacement of the methoxyl group (δ_C 55.2) in **1** by a hydroxyl group in **2** at the C-3ζ position. But for compound **3**, its 1D and 2D NMR spectra were closely related to those of **2**, except for the presence of an *O*-methyl group (δ_H/δ_C 3.68/56.0) and a hydroxyl group attached to aromatic ring in Tyr[3]. The HMBC correlation observed between methoxyl proton (δ_H 3.68) and C-3ζ (δ_C 147.5 s) indicated that the methoxyl group was positioned at C-3ζ. In addition, the hydroxyl group was deduced to be located at the C-3εa position, which was verified by the apparent downfield shift of the C-3εa signal at δ_C 148.4 together with the key HMBC correlation of H-3εb/C-3εa (Fig. 2). The absolute configurations of Ala[1], Glu[2] and Ala[4] in **2** and **3** were identified as D (*R*), L (*S*) and L (*S*), respectively. The remaining configurations of Tyr[3], Tyr[5] and Tyr[6] in **2** and **3** were deduced to be L (*S*), L (*S*) and L (*S*) respectively, from the similarities observed in NOE correlations, carbon and proton chemical shifts and proton coupling constants as compared with those of **1**. Therefore, the structures of **2** and **3** were defined as shown in Figure 1.

Rubiyunnanin F (**4**) was obtained as a white powder and gave the molecular formula $C_{48}H_{61}N_7O_{15}$ from its positive HRESIMS (976.4334 $[M+H]^+$), with 21 degrees of unsaturation. Its ^{1}H and ^{13}C NMR spectra in CD_3OD (Table 2) displayed characteristics of typical RAs and demonstrated the presence of two conformers in a ratio of 72:28. Further comparison of the 1D and 2D NMR spectra of **4** with those of RA-XII (**10**), which was a RAs glucoside isolated from *R. cordifolia* and *R. yunnanensis*,[32,2] showed many similarities except for the resonances due to those of AA[2]. The ^{1}H–^{1}H COSY correlations of H-2α/H-2β/H-2γ and HMBC correlations of H-2β and H-2γ with the carbonyl carbon at C-2δ (δ_C 177.3), together

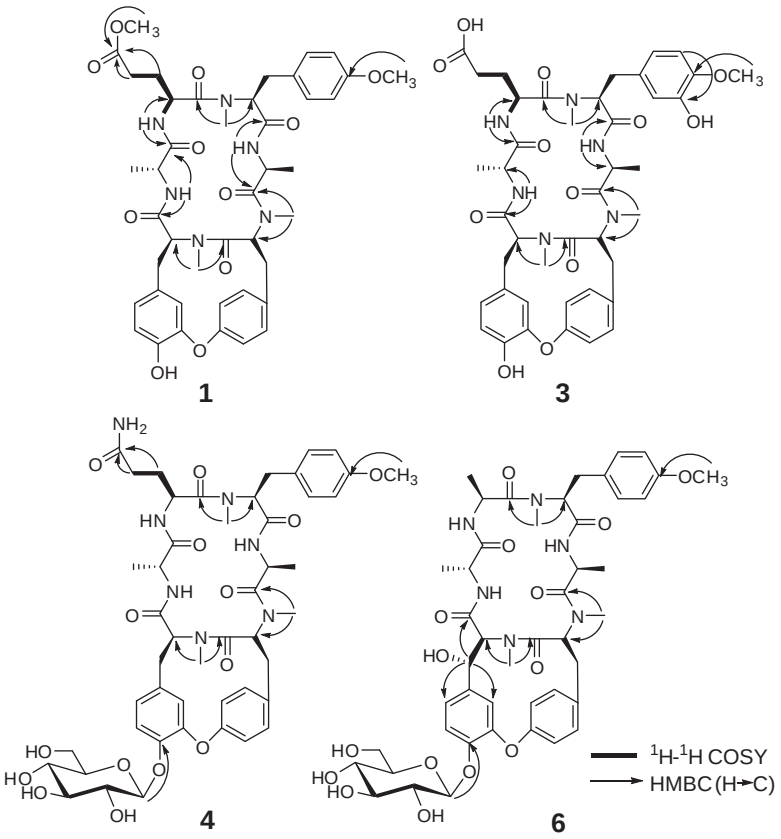

Figure 2. Selected ^{1}H–^{1}H COSY and HMBC correlations of compounds **1**, **3**, **4** and **6**.

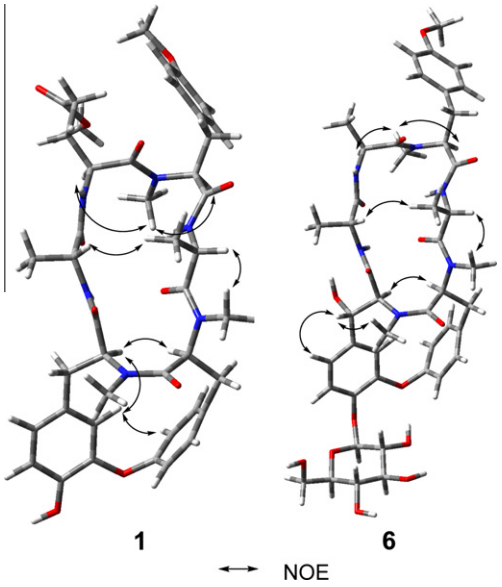

Figure 3. Selected NOE correlations of compounds **1** and **6**.

with the MS information implied that **4** was an analog of **10** whose Ala^2 was replaced by Gln^2. As for the glucopyranosyl moiety of **4**, HMBC correlation between the anomeric proton (δ_H 4.98, d, J = 7.5 Hz) (β-form) and C-6ζ indicated the linkage of the sugar group and C-6ζ (Fig. 2). The acidic hydrolysis of **4** gave D-glucose as a sugar residue, which was determined by GC analysis of its corresponding trimethylsilylated L-cysteine adduct. The absolute configurations of Ala^1 and Ala^4 were assigned as D (*R*) and L (*S*), respectively, while that of Gln^2, Tyr^3, Tyr^5 and Tyr^6 were deduced as L (*S*), L (*S*), L (*S*) and L (*S*), respectively, from the comparison of the NOE correlations, carbon and proton chemical shifts and proton coupling constants with those of **10**. Therefore, the structure of **4** was determined as shown in Figure 1.

Rubiyunnanin G (**5**) and rubiyunnanin H (**6**) were obtained as white powders. Compound **5** possessed the molecular formula $C_{45}H_{56}N_6O_{14}$ by its positive HRESIMS (*m/z* 927.3734, $[M+Na]^+$), corresponding to 21 degrees of unsaturation. Compound **6** gave the molecular formula $C_{46}H_{58}N_6O_{15}$ on the basis of its positive HRESIMS (*m/z* 957.3882, $[M+Na]^+$), indicating 21 degrees of unsaturation. The ^{1}H and ^{13}C NMR spectra of **5** and **6** in CD_3OD (Table 2) displayed characteristics of typical RAs and demonstrated the presence of two conformers in a ratio of 73:27 and 77:23, respectively. The similarities of the 1D and 2D NMR spectra of **5**, **6** and **10** showed that **5** and **6** were also RAs glucosides. The major difference between **5** and **10** was that the hydroxyl group in **5** was substituted with the methoxyl group in **10** at the C-3ζ position. In addition, the upfield shifts of C-3γ and C-3ζ from δ_C 132.2 and 159.9 in **10** to δ_C 129.6 and 158.4 in **5**, together with the downfield shift of C-3ε from δ_C 115.0 in **10** to δ_C 116.8 in **5** further corroborated this substitution. But for compound **6**, it was also structurally similar to **10** except for the presence of an oxygenated methine (δ_H/δ_C 4.66/74.3) and the absence of a methylene at δ_C 36.6 (C-6β). Based on MS information, a hydroxyl group was assigned to **6** at C-6β, which was supported by the ^{1}H–^{1}H COSY correlation of H-6β/H-6α and HMBC correlations of H-6β/C-6δa, C-6δb and Tyr^6 C=O (Fig. 2). The hydroxyl group at C-6β was determined to be α-oriented on the basis of the coupling constant of H-6β/H-6α (d, J = 8.8 Hz) and NOE correlations of H-6β/Tyr^6-NMe, H-6δa, which is the same configuration as that of RA-IV and RA-XVI (Fig. 3).[33,34] The absolute configurations of Ala^1, Ala^2 and Ala^4 in **5** and **6** were identified as D (*R*), L (*S*) and L (*S*), respectively. The remaining configurations of Tyr^3, Tyr^5 and Tyr^6 in **5** and **6** were deduced to be L (*S*),

Table 2
^{1}H NMR and ^{13}C NMR data for compounds **4–6** in CD_3OD (δ in ppm, J in Hz)

		4		**5**		**6**	
		δ_H[a]	δ_C[c]	δ_H[a]	δ_C[c]	δ_H[b]	δ_C[c]
D-Ala[1]	α	4.49 (q, 7.0)	49.0 d	4.45 (m)	48.8 d	4.48 (overlap)	48.9 d
	β	1.26 (d, 6.5)	21.4 q	1.23 (d, 7.0)	21.0 q	1.27 (overlap)	20.8 q
	C=O		173.7 s		173.4 s		173.8 s
AA[2]	α	4.80 (m)	49.5 d	4.74 (overlap)	45.6 d	4.73 (overlap)	45.5 d
	β	1.96 (m)	27.4 t	1.29 (d, 7.0)	16.4 q	1.27 (overlap)	16.6 q
	γ	2.24 (t, 7.0)	31.9 t				
	δ		177.3 s				
	C=O		173.7 s		174.6 s		174.4 s
Tyr[3]	α	3.87 (overlap)	68.8 d	3.84 (dd, 11.0, 5.0)	68.8 d	3.84 (overlap)	68.6 d
	βa	3.29 (m)	34.0 t	3.18 (dd, 13.5, 5.0)	33.7 t	3.20 (m)	33.6 t
	βb			3.25 (dd, 13.5, 11.0)			
	γ		132.3 s		129.6 s		131.6 s
	δ ∗ 2	7.11 (d, 8.5)	131.5 d	6.98 (d, 8.5)	131.4 d	7.07 (d, 8.4)	131.5 d
	ε ∗ 2	6.87 (d, 8.5)	115.1 d	6.73 (d, 8.5)	116.8 d	6.85 (d, 8.4)	115.0 d
	ζ		160.0 s		158.4 s		160.0 s
	C=O		170.9 s		171.1 s		171.0 s
	NMe	2.94 (3H, s)	40.5 q	2.92 (s)	40.3 q	2.88 (s)	40.3 q
	OMe	3.75 (3H, s)	55.7 q			3.75 (s)	55.7 q
Ala[4]	α	4.73 (m)	47.8 d	4.74 (overlap)	47.7 d	4.73 (overlap)	47.8 d
	β	1.10 (d, 6.5)	18.9 q	1.08 (d, 6.5)	18.8 q	1.12 (d, 6.4)	18.8 q
	C=O		173.0 s		173.0 s		172.6 s
Tyr[5]	α	5.43 (br d, 11.5)	55.6 d	5.46 (dd, 11.5, 3.0)	55.7 d	5.35 (dd, 11.6, 3.2)	56.0 d
	βa	2.65 (m)	37.4 t	2.68 (dd, 11.5, 3.0)	37.4 t	2.69 (dd, 11.6, 3.2)	37.5 t
	βb	3.60 (overlap)		3.57 (overlap)		3.56 (overlap)	
	γ		136.9 s		137.0 s		136.9 s
	δa	7.20 (dd, 8.5, 2.0)	134.1 d	7.21 (dd, 8.5, 2.0)	134.1 d	7.14 (overlap)	134.8 d
	δb	7.46 (br d, 8.5)	132.0 d	7.47 (dd, 8.5, 2.0)	131.8 d	7.43 (dd, 8.4, 2.0)	131.1 d
	εa	6.79 (dd, 8.5, 2.0)	125.2 d	6.81 (dd, 8.5, 2.5)	125.1 d	6.68 (dd, 8.8, 2.4)	124.9 d
	εb	7.28 (dd, 8.5, 2.0)	127.4 d	7.28 (dd, 8.5, 2.5)	127.2 d	7.38 (dd, 8.4, 2.4)	127.6 d
	ζ		159.7 s		159.8 s		160.5 s
	C=O		171.4 s		171.3 s		171.8 s
	NMe	3.06 (s)	31.1 q	3.06 (s)	31.1 q	3.05 (s)	31.1 q
Tyr[6]	α	4.68 (dd, 12.0, 3.5)	58.7 d	4.70 (dd, 11.5. 4.0)	58.6 d	4.48 (overlap)	64.4 d
	βa	3.13 (m)	36.5 t	3.08 (overlap)	36.6 t	4.66 (d, 8.8)	74.3 d
	βb	3.00 (m)		3.02 (m)			
	γ		131.6 s		132.3 s		135.8 s
	δa	6.65 (br d, 8.0)	122.7 d	6.66 (br d, 8.5)	122.6 d	6.82 (dd, 8.4, 2.0)	124.3 d
	δb	4.59 (br s)	115.8 d	4.62 (d, 1.5)	115.8 d	5.03 (d, 2.0)	117.4 d
	εa	7.08 (d, 8.0)	118.6 d	7.09 (d, 8.5)	118.7 d	7.11 (d, 8.4)	118.2 d
	εb		154.6 s		154.6 s		154.5 s
	ζ		145.4 s		145.4 s		147.3 s
	C=O		172.1 s		172.3 s		170.9 s
	NMe	2.59 (s)	30.2 q	2.61 (s)	30.1 q	2.31 (3H, s)	32.0 q
Glc	1′	4.98 (d, 7.5)	102.8 d	4.98 (d, 7.5)	102.8 d	5.01 (d, 7.6)	102.6 d
	2′	3.60 (overlap)	74.9 d	3.57 (overlap)	74.9 d	3.56 (overlap)	74.8 d
	3′	3.51 (m)	77.9 d	3.49 (m)	77.9 d	3.48 (m)	77.8 d
	4′	3.44 (overlap)	71.4 d	3.42 (overlap)	71.3 d	3.42 (overlap)	71.3 d
	5′	3.44 (overlap)	78.2 d	3.42 (overlap)	78.2 d	3.42 (overlap)	78.2 d
	6′	3.70 (dd, 12.0, 4.5)	62.5 t	3.70 (m)	62.5 t	3.69 (dd, 12.0, 4.8)	62.5 t
		3.87 (overlap)		3.88 (d, 12.0)		3.87 (overlap)	

[a] Data were measured at 500 MHz.
[b] Data were measured at 400 MHz.
[c] Data were measured at 100 MHz.

L (*S*) and L (*S*), respectively, from the similarity in their NOE correlations, carbon and proton chemical shifts and proton coupling constants, compared with those of **10**. Consequently, the structures of **5** and **6** were defined as shown in Figure 1.

Moreover, by comparing the NMR spectroscopic data, MS data and physical characteristics with the reported data in the literatures, five known RAs were identified as RA-V (**7**),[35] RA-I (**8**),[33] RA-XXIV (**9**),[21] RA-XII (**10**),[32] RY-II (**11**).[3]

2.2. Bioactivity

In the present study, the methanol extract, EtOAc-soluble fraction, *n*-BuOH-soluble fraction and H_2O-soluble fraction of *R. yunnanensis* were tested for their cytotoxicities against five cancer cell lines BEL-7402, A549, BGC-823, U251 and B16. Results indicated that the EtOAc fraction was most active against cancer cell lines (Table 3). Furthermore, all eleven RAs (**1–11**) isolated from the active EtOAc fraction were evaluated for their cytotoxicities against eleven cancer cell lines, HEPG2, BEL-7402, SMMC-7721, MDA-MB-231, DU-145, PC-3, A549, BGC-823, Hela, U251 and B16 (Table 4). Compounds **1, 7–11** exhibited significant cytotoxicities, whereas **2–6** showed weak activities. From these active constituents, RA-V (**7**) showed the best activity with nanomolar IC_{50} values. Further analysis suggested that the replacement of Ala[2] in **7** by Glu γ-methyl ester[2] in **1**, Glu[2] in **2** and **3**, Gln in **4** and **9** or Ser in **8** and **11** caused an apparent decrease in the

Table 3
The IC_{50} values of the methanol extract and its different solvent fractions on five cancer cell lines by SRB method (μg/mL)

Extract	BEL-7402	A549	BGC-823	U251	B16
Methanol extract	ND[a]	ND	ND	ND	ND
EtOAc-soluble fraction	14.32	8.16	2.18	5.32	3.66
n-Butanol-soluble fraction	ND	16.17	ND	ND	26.75
H_2O-soluble fraction	ND	ND	ND	ND	ND
Taxol	0.58	0.0008	0.02	0.02	0.11

[a] ND: no detected (>50 μg/mL).

cytotoxicity. The introduction of a hydroxyl group at the C-3εa or C-6β position, or the replacement of OMe by OH at the C-3ζ position also seems to decrease the activity. Moreover, RAs glycosides exhibited much weaker activities than their aglycons.

In a previous report, RA-V (**7**) and RA-XII (**10**) were found to show inhibitory effects on NO production and iNOS induction.[8] In this study, compounds **1–11** were also evaluated for their effects on NO production in LPS and IFN-γ-induced RAW 264.7 macrophages. All compounds showed inhibitory activities with IC_{50} values ranging from 0.05 to 12.68 μM (Table 5). Free radical NO is produced by nitric oxide synthase (NOS) as a by-product during conversion of L-arginine to L-citrulline. In the family of NOS, the inducible NOS (iNOS) is the direct target of NF-κB signaling pathway. Moreover, NF-κB is a family of dimeric transcription factors which plays vital roles in regulation of proliferation, inflammation, immune responses and apoptosis in various human pathologies.[36,37] Hence, the above results suggested that these RAs may inhibit NO production by regulating the NF-κB signaling pathway. Therefore, the effects of compounds **1–11** on NF-κB signaling pathway were examined using HEK-293-NF-κB luciferase stable cell lines. Compounds **2** and **7–10** exhibited potent inhibitory activities with IC_{50} values of 35.07, 0.03, 1.69, 12.64 and 1.18 μM, respectively (Table 5). Compound **7** has the best activity against NO production and NF-κB signaling pathway, while compound **2** has the worst activity against them. There is good correlation between the activities of these RAs against NO production and NF-κB activation (Table 5), implying that the inhibition of NO production was due to the inhibition of NF-κB signaling pathway. This is the first report demonstrating NF-κB inhibitory activity of RAs. Furthermore, compared the results in Table 4 with Table 5, it was deduced that the activities against cancer cell proliferation and NF-κB inhibition of RAs have good correlation, suggesting that the down-regulation of the NF-κB signaling pathway might play an important role in the mechanism of RAs against tumor cell growth. The more detail research on RAs and NF-κB signaling pathway is still in progress.

Table 5
Inhibition activities of NO production and NF-κB activation by compounds **1–11**

Compd	IC_{50} (μM)	
	NO[a]	NF-κB[b]
1	5.16	ND[e]
2	7.22	35.07
3	11.25	ND
4	1.77	ND
5	12.64	ND
6	12.68	ND
7	0.05	0.03
8	0.25	1.69
9	2.22	12.64
10	0.32	1.18
11	1.99	ND
MG-132[c]	0.35	
PS-341[d]		0.014

[a] Effect on NO production induced by LPS and IFN-γ in RAW 264.7 macrophages.
[b] Effect on TNF-α induced NF-κB activation in HEK-293-NK-κB luciferase stable cells.
[c] Positive control for LPS and IFN-γ stimulated NO production.
[d] Positive control for NK-κB luciferase assay.
[e] ND: no detected (>25 μg/mL).

3. Experimental

3.1. General experimental procedures

Melting points were obtained on an X-4 micromelting point apparatus. Optical rotations were measured with a Horiba SEPA-300 polarimeter. UV spectra were obtained using a Shimadzu UV-2401A spectrophotometer. IR spectra were obtained by a Tenor 27 spectrophotometer using KBr pellets. 1D and 2D NMR spectra were recorded on Bruker AM-400, DRX-500 or AV-600 spectrometers with TMS as internal standard. Coupling constants were expressed in hertz, and chemical shifts (δ) were expressed in ppm with reference to the solvent signals. Mass spectra were performed on a VG Autospec-3000 spectrometer or an API Qstar pulsa TOF spectrometer. The GC analysis was performed on an HP5890 gas chromatograph (Agilent, American) equipped with a quartz capillary column (30 mm × 0.32 mm, 0.25 μm); detection, FID. Analytical or semipreparative HPLC was performed on an Agilent 1100 liquid chromatograph with a Zorbax Eclipse-C18 (4.6 mm × 150 mm; 9.4 mm × 250 mm).

Column chromatography was performed with silica-gel (200–300 mesh, Qingdao Yu-Ming-Yuan Chemical Co. Ltd., Qingdao, China), Sephadex LH-20 (Pharmacia Fine Chemical Co., Uppsala,

Table 4
The IC_{50} values of compounds **1–11** on eleven cancer cell lines (μM)

Compd	HEPG2	BEL-7402	SMMC-7721	MDA-MB-231	DU-145	PC-3	A549	BGC-823	Hela	U251	B16
1	7.84	1.97	10.69	1.52	0.67	1.00	0.94	0.87	5.97	0.76	1.12
2	15.78	45.99	21.28	15.95	15.83	10.23	37.17	30.34	15.09	26.25	15.28
3	29.97	ND[a]	ND	37.58	43.73	54.76	45.74	ND	33.16	56.24	22.17
4	38.90	20.99	14.32	6.32	41.62	22.31	8.18	12.47	19.15	14.99	3.44
5	33.66	ND	ND	39.32	36.29	36.82	25.95	36.41	32.01	48.61	25.94
6	41.35	ND	35.97	ND	ND	ND	32.82	ND	48.17	42.31	29.24
7	0.14	0.08	0.13	0.01	0.01	0.05	0.06	0.01	0.04	0.001	0.001
8	1.01	2.02	2.41	0.16	0.59	0.80	0.42	0.39	0.91	1.96	0.22
9	8.01	8.45	9.09	1.44	2.03	3.66	2.85	3.26	6.16	10.81	1.01
10	8.68	7.49	8.82	5.97	2.88	6.55	1.82	3.71	5.18	10.03	1.40
11	12.76	11.45	12.97	8.57	10.65	14.40	5.02	6.91	3.52	8.20	2.89
Taxol	0.11	1.07	ND	ND	0.01	ND	0.001	0.02	0.07	0.03	0.04
CPT			0.02	0.33		16.24					

[a] ND: no detected (>50 μg/mL).

Sweden), Lichroprep RP-18 gel (40–63 μM, Merck, Darmstadt, Germany). Fractions were monitored by TLC (GF254, Qingdao Yu-Ming-Yuan Chemical Co. Ltd., Qingdao, China), and spots were visualized by heating Si gel plates spray with 5% H_2SO_4 in EtOH or 2% ninhydrin reagent. The plate was handed in a sealed glass vessel with about 1 mL of concentrated HCl and hydrolyzed in a drying incubator (110 °C) for 1 h, and orange spots were visualized by spraying with 2% ninhydrin reagent.[38]

3.2. Plant material

The roots of *R. yunnanensis* were commercially purchased from the Yunnan Lv-Sheng Pharmaceutical Co. Ltd., Kunming, China. The material was identified by Prof. Su-Gong Wu at Kunming Institute of Botany. A voucher specimen (No. Wu20070905) has been deposited in the Herbarium of Kunming Institute of Botany, Chinese Academy of Sciences.

3.3. Cell lines and reagents

Eleven cancer cell lines, HEPG2 (human hepatocellular carcinoma), BEL-7402 (human hepatocellular carcinoma), SMMC-7721 (human hepatocellular carcinoma), MDA-MB-231 (human breast carcinoma), DU-145 (human prostate carcinoma), PC-3 (human prostate carcinoma), A549 (human non-small cell lung carcinoma), BGC-823 (human gastric carcinoma), Hela (human cervical carcinoma), U251 (human golima) and B16 (murine melanoma) were used in our experiments. All cancer cell lines were cultured in RPMI 1640 medium supplemented with 10% FBS under a humidified atmosphere of 5% CO_2 at 37 °C. The murine monocytic macrophage cell lines RAW 264.7 were cultured in RPMI 1640 medium (Hyclone, USA) with 10% FBS under a humidified atmosphere of 5% CO_2 at 37 °C. pNF-κB-Luc vector (Clontech Laboratories, Inc.) and pCDNA3.1(−) (Invitrogen, USA) were cotransfected into human embryonic kidney (HEK)-293 cells with a 10:1 ratio, and HEK-293-NF-κB luciferase stable cell lines were established with G418 selection and cultured in HG-DMEM medium (Gibco, USA) with 10% FBS and supplemented with 700 μg/mL G418 under a humidified atmosphere of 5% CO_2 at 37 °C.

Roswell Park Memorial Institute 1640 (RPMI 1640) (Sigma–Aldrich, Milan, Italy), fetal bovine serum (FBS), sulforhodamine B (SRB) (Sigma–Aldrich), trichloroacetic acid (TCA) and Tris solution were used for the cytotoxic assay. Griess reagent (1:1, v/v, 1% sulfanilamide and 0.1% *N*-(1-naphthyl) ethylenediamine dihydrochloride in 2.5% H_3PO_4), MTT (3-(4,5-dimethylthiazol-2-yl)-2,5-diphenyltetrazoliun bromide) (Sigma–Aldrich), lipopolysaccharide (LPS), interferon-gamma (IFN-γ) were used for measurement of NO. The single luciferase reporter assay system (Promega, USA) and TNF-α were used for NF-κB luciferase assay.

3.4. Extraction and isolation

The air-dried and powdered roots of *R. yunnanensis* (100 kg) were extracted three times with methanol (3 × 100 L). After removal of the solvent under vacuum, the methanol extract (21 kg) was suspended in water and partitioned successively with ethyl acetate and *n*-butanol, respectively. The EtOAc part (6.4 kg) was subjected to silica gel column chromatography eluted with $CHCl_3$–MeOH (1:0, 95:5, 9:1, 8:2, 0:1) to afford five fractions. Fractions which contained cyclopeptides (1.2 kg, $CHCl_3$–MeOH, 95:5, 9:1, 8:2) were combined and again rechromatographed on a silica gel column eluting with a $CHCl_3$–MeOH gradient system (70:1–8:2) to yield six fractions (Fr.1–Fr.6).

Fr.1 (139 g) was applied to silica gel column chromatography (CC) using petroleum ether–acetone (7:3–0:1) to furnish five subfractions (Fr.1-1 to Fr.1-5). Fr.1-4 (30 g) was separated using Sephadex LH-20 ($CHCl_3$–MeOH, 1:1) and then purified over repeated silica gel H eluting with petroleum ether–acetone (6:4) to afford RA-V (**7**) (4 g, 0.004%).

Fr.2 (257 g) was chromatographed over silica gel using $CHCl_3$–MeOH gradient system (95:5–9:1) to give seven subfractions (Fr.2-1 to Fr.2-7). Fr.2-4 (104 g) was subjected to a reversed-phase column (RP-18) eluting with MeOH–H_2O (20–90%) to afford six subfractions (Fr.2-4-1 to Fr.2-4-6). Fr.2-4-2 (18 g) were separated by Sephadex LH-20 ($CHCl_3$–MeOH, 1:1) and then subjected to RP-18 column (MeOH–H_2O, 30–50%) to afford RA-I (**8**) (145 mg, 0.00015%). Then Fr.2-4-5 was also passed through Sephadex LH-20 ($CHCl_3$–MeOH, 1:1), RP-18 column (MeOH–H_2O, 20–40%), and repeated silica gel H column ($CHCl_3$–MeOH, 20:1–10:1) to yield rubiyunnanin C (**1**) (34 mg, 0.000034%).

Fr.3 (94 g) was subjected to a silica gel column using $CHCl_3$–MeOH (70:1–9:1) to furnish five subfractions (Fr.3-1 to Fr.3-5). Fr.3-3 (12 g) was chromatographed over a silica gel column using petroleum ether–acetone (1:1–0:1), followed by a Sephdex LH-20 column ($CHCl_3$–MeOH, 1:1) and then further purified by repeated silica gel H eluting with $CHCl_3$–MeOH (20:1) to give RA-XXIV (**9**) (290 mg, 0.00029%).

Fr.4 (365 g) was separated by a silica gel column using EtOAc–MeOH (20:1–8:2) to yield four subfractions (Fr.4-1 to Fr.4-4). Fr.4-3 (50 g) was separated by Sephdex LH-20 ($CHCl_3$–MeOH, 1:1) and followed by silica gel ($CHCl_3$–MeOH, 95:5–0:1) to afford seven subfractions (Fr.4-3-1 to Fr.4-3-7). Fr.4-3-5 (21 g) was further separated by repeated RP-18 (MeOH–H_2O, 40–60%) and led to the isolation of RA-XII (**10**) (6 g, 0.006%). Fr. 4-3-7 (46 mg) was separated by ODS HPLC (33% ACN, 4‰ TFA) to obtain rubiyunnanin D (**2**) (9 mg, 0.000009%) and rubiyunnanin E (**3**) (29 mg, 0.000029%).

Fr.5 (87 g) was divided into four subfractions (Fr.5-1 to Fr.5-4) by CC over silica gel eluting with gradient $CHCl_3$–MeOH (95:5–0:1). Fr. 5-3 (35 g) was subjected to CC over silica gel using EtOAc–MeOH (20:1–8:2) to give four subfractions (Fr.5-3-1 to Fr.5-3-4). Then Fr. 5-3-2 (4.5 g) and Fr. 5-3-4 (6 g) were separated by Sephadex LH-20 ($CHCl_3$–MeOH, 1:1) and subjected to RP-18 colum (MeOH–H_2O, 20–50%) to afford cyclopeptides-rich fractions, respectively. RY-II (**11**) (57 mg, 0.000057%) was finally purified by ODS HPLC (23% ACN, 4‰ TFA) from subfraction Fr. 5-3-2. Rubiyunnanin G (**5**) (6 mg, 0.000006%) and rubiyunnanin H (**6**) (8 mg, 0.000008%) were purified by ODS HPLC (40% ACN, 4‰ TFA) from subfraction Fr. 5-3-4.

Fr.6 (151 g) was subjected to a silica gel column using $CHCl_3$/MeOH/H_2O (9:1:0.1–8:2:0.2) to furnish four subfractions (Fr.6-1 to Fr.6-4). Fr.6-3 (27 g) was then applied to a silica gel column using EtOAc–MeOH (20:1–8:2) to afford cyclopeptides-rich fraction (Fr.6-3-2), then separated by RP-18 colum (MeOH–H_2O, 10–40%) to afford six subfractions (Fr.6-3-2-1 - Fr.6-3-2-6). Rubiyunnanin F (**4**) (22 mg, 0.000022%) was purified by ODS HPLC (28% ACN, 4‰ TFA) from subfraction Fr. 6-3-2-1.

Rubiyunnanin C (**1**): White crystal; mp 253–254 °C; $[\alpha]_D^{27}$ −221.0 (*c* 0.11, $CHCl_3$/MeOH = 1:1); UV (MeOH) λ_{max} (log ε) 203 (4.80), 277 (3.78) nm; IR (KBr) ν_{max} 3414, 2937, 1737, 1660, 1514, 1445, 1239, 1209, 1096, 838, 803 cm^{-1}; for ^1H and ^{13}C NMR data, see Table 1; positive FABMS *m/z* 829 (100) $[M+H]^+$; positive HRFABMS *m/z* 828.3713 $[M]^+$, cacld for $C_{43}H_{52}N_6O_{11}$, 828.3694.

Rubiyunnanin D (**2**): Amorphous powder; $[\alpha]_D^{23}$ −149.7 (*c* 0.57, MeOH); UV (MeOH) λ_{max} (log ε) 203 (4.69), 276 (3.70) nm; IR (KBr) ν_{max} 3421, 2938, 1659, 1516, 1448, 1203, 1138, 838, 722 cm^{-1}; for ^1H and ^{13}C NMR data, see Table 1; positive FABMS *m/z* 801 (10) $[M+H]^+$; positive HRESIMS *m/z* 823.3259 $[M+Na]^+$, cacld for $C_{41}H_{48}N_6O_{11}Na$, 823.3278.

Rubiyunnanin E (**3**): Amorphous powder; $[\alpha]_D^{23}$ −124.5 (*c* 0.58, MeOH); UV (MeOH) λ_{max} (log ε) 204 (4.81), 280 (3.87) nm; IR (KBr) ν_{max} 3426, 2938, 1664, 1515, 1446, 1204, 1134, 839, 801,

722 cm^{-1}; for ^1H and ^{13}C NMR data, see Table 1; positive FABMS *m/z* 831 (50) $[M+H]^+$; positive HRESIMS *m/z* 853.3391 $[M+Na]^+$, cacld for $C_{42}H_{50}N_6O_{12}Na$, 853.3384.

Rubiyunnanin F (**4**): Amorphous powder; $[\alpha]_D^{25}$ −182.5 (*c* 0.37, MeOH); UV (MeOH) λ_{max} (log ε) 203 (4.87), 276 (3.80) nm; IR (KBr) ν_{max} 3423, 2932, 1663, 1512, 1447, 1414, 1248, 1208, 1075, 839, 803 cm^{-1}; for ^1H and ^{13}C NMR data, see Table 2; positive FABMS *m/z* 976 (92) $[M+H]^+$, 814 (13) $[M+2H-Glc]^+$; positive HRESIMS *m/z* 976.4334 $[M+H]^+$, cacld for $C_{48}H_{62}N_7O_{15}$, 976.4303.

Rubiyunnanin G (**5**): Amorphous powder; $[\alpha]_D^{28}$ −127.3 (*c* 0.11, MeOH); UV (MeOH) λ_{max} (log ε) 203 (4.57), 277 (3.53) nm; IR (KBr) ν_{max} 3440, 2936, 1658, 1640, 1517, 1449, 1207, 838, 810 cm^{-1}; for ^1H and ^{13}C NMR data, see Table 2; positive FABMS *m/z* 905 (24) $[M+H]^+$; positive HRESIMS *m/z* 927.3734 $[M+Na]^+$, cacld for $C_{45}H_{56}N_6O_{14}Na$, 927.3752.

Rubiyunnanin H (**6**): Amorphous powder; $[\alpha]_D^{27}$ −244.0 (*c* 0.12, MeOH); UV (MeOH) λ_{max} (log ε) 203 (4.81), 276 (3.83) nm; IR (KBr) ν_{max} 3424, 2933, 1657, 1640, 1512, 1248, 1075, 826 cm^{-1}; for ^1H and ^{13}C NMR data, see Table 2; positive FABMS *m/z* 935 (95) $[M+H]^+$; positive HRESIMS *m/z* 957.3882 $[M+Na]^+$, cacld for $C_{46}H_{58}N_6O_{15}Na$, 957.3857.

3.5. Marfey's analysis of the absolute configuration of amino acids

Hydrolysis of compounds **1–6** (1 mg each) were achieved in separate experiments, by the addition of 1 mL of 6 N HCl at 115 °C for 18 h. The hydrolyzate was evaporated to dryness under a stream of N_2 to remove traces of HCl. Then, the resultant hydrolyzate was redissolved in 900 μL of acetone, thereafter, 1 M $NaHCO_3$ (20 μL) and a 1% solution of Nα-(2,4-dinitro-5-fluorophenyl)-L-alaninamide (L-FDAA, Marfey's reagent, Sigma, 100 μL) in acetone were added, and the mixture was heated at 40 °C for 1 h. The reaction mixture was cooled to RT and quenched by addition of 2 N HCl (10 μL), dried, and dissolved in 50% aqueous CH_3CN (600 μL). Five micro liters of the FDAA derivative was analyzed by HPLC using a C18 column (Agilent, 4.6 mm × 150 mm, 5 μm, Zorbax Eclipse-C_{18}) maintained at 30 °C. Aqueous CH_3CN containing 4‰ TFA was used as the mobile phase with linear gradient elution (20–35%, 40 min) at a flow rate of 1 mL/min. FDAA-derivatived amino acids were detected by absorption at 340 nm.

To 50 μL of a 50 mM aqueous solution of D and L-configurations of Ala (no hydrolysis), Glu (no hydrolysis) and Glu (hydrolysis with 6 N HCl, 115 °C, 18 h) were added 1 M $NaHCO_3$ (20 μL) and a 1% solution of L-FDAA (100 μL) in acetone, respectively. Each mixture was heated at 40 °C for 1 h. The reaction mixture was cooled to RT and quenched by the addition of 2 N HCl (10 μL). It was dried, dissolved in 50% aqueous CH_3CN (600 μL). Then 5 μL of the FDAA derivative was analyzed by HPLC.

The retention times (min) of the L-FDAA derivatives of standard amino acids were observed to be L-Ala (14.275), D-Ala (19.387), L-Glu (11.273), D-Glu (13.179) L-Glu hydrolyzed with 6 N HCl (11.304, 18.114) and D-Glu hydrolyzed with 6 N HCl (13.229, 23.685), respectively. The retention times (min) of the L-FDAA derivatives of acid hydrolysates of compounds **1–6** were summarized as follows: **1**, L-Ala (14.334), D-Ala (19.465); **2**, L-Ala (14.391), L-Glu (18.218), D-Ala (19.522); **3**, L-Ala (14.388), L-Glu (18.212), D-Ala (19.512); **4**, L-Ala (14.248), D-Ala (19.578); **5**, L-Ala (14.395), D-Ala (19.710); **6**, L-Ala (14.372), D-Ala (19.794).

3.6. Acidic hydrolysis of compound 4

Compound **4** (10 mg) was hydrolyzed with 2 M HCl-dioxane (1:1, 4 mL) under reflux at 80 °C for 6 h. The reaction mixture was extracted with $CHCl_3$ three times (2 mL × 3). The aqueous layer was neutralized with 2 M NaOH and then dried to give a monosaccharide mixture. The dry powder was dissolved in pyridine (2 mL), L-cysteine methyl ester hydrochloride (1.5 mg) was added, and the mixture was heated at 60 °C for 1 h. Thereafter, trimethylsilylimidazole (1.5 mL) was added to the reaction mixture in ice water and kept at 60 °C for 30 min. The mixture was directly subjected to GC analysis under the following conditions: column temperature 180–280 °C; programmed increase, at 3 °C/min; carrier gas, N_2 (1 mL/min); injector and detector temperature, 250 °C; injection volume, 4 μL; and split ratio, 1:50. The configuration of D-glucose for compound **4** was determined by comparing the retention time with the derivative of authentic sample (D-glucose: 18.074 min).

Acknowledgements

This work was supported by the National Natural Science Foundation of China (30725048), National Basic Research Program of China (2009 CB522300), the Fund of Chinese Academy of Sciences (KSCX2-YW-R-177), the Innovative Group Program from the Science and Technology Department of Yunnan Province (2008OC011) and the Fund of State Key Laboratory of Phytochemistry and Plant Resources in West China, Kunming Institute of Botany, Chinese Academy of Sciences. We thank Mrs. Ogunlana Olubanke and Dr. Abiodun Humphrey Adebayo for proof reading the manuscript.

Supplementary data

Supplementary data associated with this article can be found, in the online version, at doi:10.1016/j.bmc.2010.10.019. These data include MOL files and InChiKeys of the most important compounds described in this article.

References and notes

1. *Dian Nan Ben Cao*; Lan, M., Ed.; Yunnan People's Publishing House: Kunming, 1978; pp 349–351.
2. Zou, C.; Hao, X. J.; Zhou, J. *Acta Bot. Yunnanica* **1993**, *15*, 399.
3. He, M.; Zou, C.; Hao, X. J.; Zhou, J. *Acta Bot. Yunnanica* **1993**, *15*, 408.
4. Shen, X. Y.; Wu, H. M.; He, M.; Hao, X. J.; Zhou, J. *Acta Chem. Sinica* **1996**, *54*, 1194.
5. Chen, Y. Q.; Luo, Y. R. *Youji Huaxue* **1991**, *11*, 523.
6. Liou, M. J.; Wu, P. L.; Wu, T. S. *Chem. Pharm. Bull.* **2002**, *50*, 276.
7. Liou, M. J.; Teng, C. M.; Wu, T. S. *J. Chin. Chem. Soc.* **2002**, *49*, 1025.
8. Tao, J.; Morikawa, T.; Ando, S.; Matsuda, H.; Yoshikawa, M. *Chem. Pharm. Bull.* **2003**, *51*, 654.
9. Zou, C.; Hao, X. J.; Chen, C. X.; Zhou, J. *Acta Bot. Yunnanica* **1992**, *14*, 114.
10. Zou, C.; Hao, X. J.; Chen, C. X.; Zhou, J. *Acta Bot. Yunnanica* **1993**, *15*, 89.
11. Xu, X. Y.; Zhou, J. Y.; Fang, Q. C. *J. Chin. Pharm. Sci.* **1995**, *4*, 157.
12. Zou, C.; Hao, X. J.; Chen, C. X.; Zhou, J. *Acta Bot. Yunnanica* **1999**, *21*, 256.
13. Liou, M. J.; Wu, T. S. *J. Nat. Prod.* **2002**, *65*, 1283.
14. Morikawa, T.; Tao, J.; Ando, S.; Matsuda, H.; Yoshikawa, M. *J. Nat. Prod.* **2003**, *66*, 638.
15. Itokawa, H.; Takeya, K.; Mori, N.; Hamanaka, T.; Sonobe, T.; Mihara, K. *Chem. Pharm. Bull.* **1984**, *32*, 284.
16. Itokawa, H.; Takeya, K.; Mori, N.; Sonobe, T.; Serisawa, N.; Hamanaka, T.; Mihashi, S. *Chem. Pharm. Bull.* **1984**, *32*, 3216.
17. Tan, N. H.; Zhou, J. *Chem. Rev.* **2006**, *106*, 840.
18. Jolad, S. D.; Hoffmann, J. J.; Torrance, S. J.; Wiedhopf, R. M.; Cole, J. R.; Arora, S. K.; Bates, R. B.; Gargiulo, R. L.; Kriek, G. R. *J. Am. Chem. Soc.* **1977**, *99*, 8040.
19. Lee, J. E.; Hitotsuyanagi, Y.; Kim, I. H.; Hasuda, T.; Takeya, K. *Bioorg. Med. Chem. Lett.* **2008**, *18*, 808.
20. Lee, J. E.; Hitotsuyanagi, Y.; Takeya, K. *Tetrahedron* **2008**, *64*, 4117.
21. Lee, J. E.; Hitotsuyanagi, Y.; Fukaya, H.; Kondo, K.; Takeya, K. *Chem. Pharm. Bull.* **2008**, *56*, 730.
22. Fan, J. T.; Chen, Y. S.; Xu, W. Y.; Du, L. C.; Zeng, G. Z.; Zhang, Y. M.; Su, J.; Li, Y.; Tan, N. H. *Tetrahedron Lett.* **2010**. doi:10.1016/j.tetlet.2010.07.066.
23. Tobey, R. A.; Orlicky, D. J.; Deaven, L. L.; Rall, L. B.; Kissane, R. *J. Cancer Res.* **1978**, *38*, 4415.
24. Zalacain, M.; Zaera, E.; Vazquez, D.; Jimenez, A. *FEBS Lett.* **1982**, *148*, 95.
25. Sirdeshpande, B. V.; Toogood, P. L. *Bioorg. Chem.* **1995**, *23*, 460.
26. Fujiwara, H.; Saito, S. Y.; Hitotsuyanagi, Y.; Takeya, K.; Ohizumi, Y. *Cancer Lett.* **2004**, *209*, 223.
27. Koizumi, T.; Abe, M.; Yamakuni, T.; Ohizumi, Y.; Hitotsuyanagi, Y.; Takeya, K.; Sato, Y. *Cancer Sci.* **2006**, *97*, 665.

28. Du, L. C.; Tan, N. H.; Xu, W. Y.; Lou, L. L. *Acta Bot. Yunnanica* **2009**, *31*, 374.
29. Bates, R. B.; Cole, J. R.; Hoffmann, J. J.; Kriek, G. R.; Linz, G. S.; Torrance, S. J. *J. Am. Chem. Soc.* **1983**, *105*, 1343.
30. Morita, H.; Kondo, K.; Hitotsuyanagi, Y.; Takeya, K.; Itokawa, H.; Tomioka, N.; Itai, A.; Iitaka, Y. *Tetrahedron* **1991**, *47*, 2757.
31. Marfey, P. *Carlsberg Res. Commun.* **1984**, *49*, 591.
32. Morita, H.; Yamamiya, T.; Takeya, K.; Itokawa, H. *Chem. Pharm. Bull.* **1992**, *40*, 1352.
33. Itokawa, H.; Takeya, K.; Mori, N.; Sonobe, T.; Mihashi, S.; Hamanaka, T. *Chem. Pharm. Bull.* **1986**, *34*, 3762.
34. Takeya, K.; Yamamiya, T.; Morita, H.; Itokawa, H. *Phytochemistry* **1993**, *33*, 613.
35. Itokawa, H.; Takeya, K.; Mihara, K.; Mori, N.; Hamanaka, T.; Sonobe, T.; Iitaka, Y. *Chem. Pharm. Bull.* **1983**, *31*, 1424.
36. Pahl, H. L. *Oncogene* **1999**, *18*, 6853.
37. Karin, M.; Cao, Y.; Greten, F. R.; Li, Z. W. *Nat. Rev. Cancer* **2002**, *2*, 301.
38. Zhou, J.; Tan, N. H. *Chin. Sci. Bull.* **2000**, *45*, 1825.